

Effect of Organic Buffer Layer on Performance of Pentacene Field-Effect Transistor Fabricated on Natural Mica Gate Dielectric

Akira Matsumoto, Ryo Onoki, Susumu Ikeda¹, Koichiro Saiki¹, and Keiji Ueno*

Department of Chemistry, Saitama University, 255 Shimo-Okubo, Sakura-ku, Saitama 338-8570, Japan

¹Department of Complexity Science and Engineering, The University of Tokyo, 5-1-5 Kashiwanoha, Kashiwa, Chiba 277-8561, Japan

The mobility of pentacene-based organic field-effect transistors (OFETs) fabricated on natural mica substrates has been highly improved using polymethylmethacrylate (PMMA) or octadecyltrimethoxysilane (OTMS) as a buffer layer between the mica dielectric and the pentacene active layer. The field-effect mobility increased from 2.4×10^{-3} to 0.14 or 0.31 $\text{cm}^2 \cdot \text{V}^{-1} \cdot \text{s}^{-1}$ by inserting the PMMA or OTMS buffer layer, respectively. The suppression of the unfavorable effect of potassium ions using the OTMS buffer layer confirmed the feasibility of using natural mica as a transparent gate dielectric of organic field-effect transistors.

KEYWORDS: organic field-effect transistor, mica, pentacene, layered material, self-assembled monolayer, carrier transport

*E-mail address: kei@chem.saitama-u.ac.jp

Recently, the organic field-effect transistor (OFET) has been widely studied and its device performance has been considerably improved.^{1,2)} In many studies of OFETs, the organic semiconductor layer is formed on amorphous substrates such as thermally grown SiO_x on highly doped Si, organic polymer films, and sputtered oxide films. All these substrates are amorphous or polycrystalline; thus, single-crystalline organic films never grow on them, causing poorer performance compared with single-crystalline inorganic semiconductors. The growth of a single-crystalline organic film, however, can be expected if an appropriate material is chosen as a substrate. Indeed, the epitaxial growth of organic films on many layered material substrates such as MoS₂, mica, graphite, and GeS has been reported.³⁻⁷⁾ It has been found that the initial organic layer on the gate dielectric surface mainly dictates the working characteristics.^{8,9)} Thus, the improvement of the crystallinity of the initial organic layer is expected to decrease the number of defects or grain boundaries and enhances OFET performances.

In a previous work, we fabricated pentacene OFETs on a single-crystalline natural mica substrate.¹⁰⁾ Mica is a typical insulator with a layer structure that can easily be cleaved to a thin film, the thickness of which is thin enough to work as a gate dielectric of OFETs. The epitaxial growth of the pentacene film on mica was actually observed by reflection high-energy electron diffraction (RHEED) analysis even at room temperature (RT, about 25°C). Atomic force microscopy (AFM) and X-ray diffraction (XRD) observations also revealed the growth of good pentacene films comparable to those on a SiO_x gate substrate. Pentacene OFETs on the mica gate dielectric, however, showed quite poor FET performances. The highest field-effect mobility was as low as $2.4 \times 10^{-3} \text{ cm}^2 \cdot \text{V}^{-1} \cdot \text{s}^{-1}$, and the best on-off ratio was only 4.3. We considered that potassium ions on the cleaved surface of mica functioned as the carrier scattering center and obstructed the carrier transport in the organic active layer.

In the present work, a cast-coated film of polymethylmethacrylate (PMMA) or a self-assembled monolayer (SAM) of octadecyltrimethoxysilane (OTMS) was inserted

between the mica gate dielectric surface and the pentacene film in order to evaluate the effect of potassium ions on carrier transport. The insertion of the buffer layer can separate the pentacene active layer from the potassium ions on the cleaved surface of mica. Then, we expect to improve OFET performances by reducing the unfavorable effect of the potassium ions on the carrier transport in the pentacene active layer. In the case of PMMA, we changed the film thickness and evaluated the effect of the separation of potassium ions from the active layer. In the case of OTMS, vertically aligned molecules were expected to cause additional effects, although the measured thickness of the SAM was only 2.5 nm, far thinner than the PMMA film.

A natural mica (muscovite) substrate was cleaved using adhesive tape in atmosphere to approximately 1 - 5 μm in thickness, and the cleaved surface was coated with PMMA or OTMS. PMMA (Sigma-Aldrich) was dissolved in toluene and the resulting solution was dropped onto the mica surface. Subsequently, the coated mica specimen was dried in air at 120°C for 3 h. The weight percent concentration of the PMMA solution was varied from 0.5 to 2.0 weight % (wt%) to change the film thickness. The thickness of the PMMA film was estimated by measuring the capacitance of the cast-coated film on a highly doped metallic Si substrate.

An OTMS-SAM was fabricated by a gas-phase process; a cleaved mica substrate and a glass tube containing OTMS liquid (Tokyo Kasei, >85% purity) were separately set in a tightly sealed Teflon vessel that was heated at 100°C for 1 h in a drying oven. During the heating process, the silane-coupling reaction of the vaporized OTMS molecules proceeds and an ordered SAM grows on the mica surface.

As-purchased pentacene (Sigma-Aldrich, 98% purity) was evaporated from a Knudsen cell onto the coated surfaces of mica for 2 h under a high-vacuum condition (ca. 10^{-5} Pa). The substrate temperature was kept at RT. Finally, source and drain electrodes of Au were

formed by thermal deposition through a metal shadow mask placed in front of the pentacene film. The channel length and width of the top-contact OFET were 0.1 and 1.0 mm, respectively. A conductive silver paste (Dotite S-550) applied to the back of the mica dielectric was used as the gate electrode. The capacitance of the gate dielectric, which is a series of the mica substrate and buffer film, was measured using an impedance meter (Tecpel LCR612) at 120 Hz. Current-voltage measurements of OFETs were performed in a vacuum desiccator (ca. 1 Pa) using two picoammeter/voltage source units (Keithley 6487). The morphology and the crystallinity of pentacene films were investigated by AFM, and XRD and RHEED analyses.

Figure 1 shows AFM images of a PMMA-coated mica substrate, an OTMS-coated mica substrate, and pentacene films grown on these substrates at room temperature for 2 h. The thicknesses of the PMMA and OTMS films were 85 and 2.5 nm, respectively. The root mean square values of the surface roughness of the mica, PMMA/mica, and OTMS/mica substrates were 0.27, 0.56 and 0.37 nm, respectively. The pentacene domains deposited on the PMMA- and OTMS-coated substrates at RT had a rounded shape and were smaller than those on the bare mica substrate¹⁰, about 1/2 - 1/3 in size. The surface roughness of the PMMA film and the shape of the pentacene domains on PMMA did not change when PMMA film thickness was increased. There were small holes in the OTMS film, but the other film surface was as flat as the mica substrate.

XRD measurements revealed that the pentacene films grown at RT on the PMMA/mica and OTMS/mica substrates consisted of a single phase, so called a “thin-film” phase.¹¹⁾ Thus, the out-of-plane ordering of the pentacene films did not change owing to the surface modification of mica substrates. On the other hand, RHEED measurements revealed different results for the in-plane ordering. No streak pattern was observed for the pentacene films on the PMMA- or OTMS-coated substrate, while streak patterns indicating epitaxial

growth were observed on a bare mica surface.¹⁰⁾ Thus, it is suggested that the in-plane ordering of the pentacene films on the coated mica substrates was poorer than that on the bare mica substrate.

Figure 2 shows the transfer characteristics of the pentacene OFETs fabricated on mica substrates coated with PMMA films having various thicknesses. Here, the drain voltage (V_D) was set to 200 V. It should be noted that the capacitance of the gate dielectric decreases with increasing PMMA thickness, causing a proportional decrease in drain current (I_D). In addition, the thickness of the mica substrate differs from sample to sample. Therefore, I_D must be normalized in order to accurately elucidate the effect of PMMA thickness on drain current. Thus, the vertical axis in Fig. 2 is normalized by dividing the measured I_D by the value of the gate capacitance per unit gate area (F/m^2) for each OFET sample. The real gate capacitance per unit area was about 15 - 25 $\mu F/m^2$. As shown in Fig. 2, the thicker the PMMA film is, the more *normalized* I_D flows in the pentacene channel in OFETs fabricated at RT. Thus, it is suggested that the PMMA film inserted between the mica and the pentacene film can improve OFET performances, and its thickness plays an important role in this improvement.

Figure 3 shows the output characteristics of two pentacene OFETs: on a bare mica surface (a) and on a 280-nm-thick PMMA-coated mica surface (b). I_D was very low and no saturation region was observed on the bare mica gate dielectric, while I_D was markedly increased on the PMMA-coated mica gate. The transfer characteristics of both OFETs are also shown in Fig. 3(c). From these OFET characteristics, performance values such as field-effect mobility (μ), on/off current ratio, and threshold voltage (V_{th}) were obtained. The field-effect mobility (μ) was evaluated in the linear region using eq. (1):

$$\frac{\partial I_D}{\partial V_G} = \frac{WC\mu}{L} V_D, \quad (1)$$

where V_G is the gate voltage, V_D is the drain voltage ($V_D \ll (V_G - V_{th})$), W is the channel width,

L is the channel length, and C is the measured gate capacitance per unit area¹. Table I summarizes these performance values of the pentacene OFETs fabricated on bare and PMMA-coated mica substrates. The highest mobility ($1.4 \times 10^{-1} \text{ cm}^2 \cdot \text{V}^{-1} \cdot \text{s}^{-1}$) and an on/off ratio of 197 were obtained with the thickest (280 nm) PMMA film. The growth features of the pentacene films on the PMMA/mica substrates observed by AFM and XRD analysis, however, were independent of the thickness of the PMMA films. Thus, it is concluded that the screening effect of the PMMA film hides the potassium ions from the pentacene active layer and that the thicker PMMA film can more effectively block the ionic influence and improve OFET performances.

Figures 4(a) and 4(b) show the output characteristics and transfer characteristics of a pentacene OFET on an OTMS-coated mica substrate, respectively. Although the thickness of the OTMS-SAM fabricated on mica is very small (about 2.5 nm, measured by AFM), a high I_D was observed corresponding to that of the 280-nm-thick PMMA-coated mica substrate. The field-effect mobility in the linear region calculated using eq. (1) was $3.1 \times 10^{-1} \text{ cm}^2 \cdot \text{V}^{-1} \cdot \text{s}^{-1}$, which is the best value among any of the pentacene OFETs fabricated on the mica substrates with and without the buffer layer, as summarized in Table I.

The difference between PMMA and OTMS in terms of the ability to improve OFET performances can be explained as follows. In the case of drop-casted PMMA, a randomly extended amorphous-like polymer film is fabricated on the mica substrate, and the entire PMMA film has almost no polarization, as schematically shown in Fig. 5(a). Such a nonpolar PMMA film has poor ability to shield the pentacene layer from the potassium ions on the mica surface. Therefore, a thicker PMMA film is required to improve OFET performances. In the case of OTMS, on the contrary, every molecule is vertically aligned, and a highly ordered SAM can be deposited on the mica surface through the silane-coupling reaction, as shown in Fig. 5(b). Then, slightly polarized OTMS molecules¹²⁾ are arranged in parallel, and the entire buffer layer acts as an electric double layer. According to ref. 12, the

calculated dipole moment directed normally to the substrate for an OTMS-SAM deposited on SiO₂/Si substrate is 0.429 Debye. Therefore, the pentacene layer can be effectively screened from the potassium ions on the mica surface. The present OTMS treatment is still insufficient because there are some holes remaining, as shown in Fig. 1(c). In these holes the bare mica surface might be exposed. If the coverage of OTMS can be improved, the mobility is expected to increase further.

Here, it must be noted that the surfaces of these buffer layers have no *in-plane* ordering. Thus, the use of buffer films on the mica substrate generally loses the merit of the in-plane ordering of the pentacene film at the present stage. However, the advantage of the mica dielectric still remains. First, natural mica is a low-cost material. Second, mica is transparent, and coating of a very thin OTMS layer on mica, as examined in the present work, hardly changes its optical property. The metal electrode deposited on the backside is typically 20 - 30 nm; thus, the transparency of the structure is still maintained. Therefore, the organic FET fabricated on the OTMS-coated mica could easily be applied to optical devices without concern over the limitation of natural resources, for example, In.¹³⁾ Third, there remains the possibility of fabricating an in-plane ordered organic active layer using a single-crystalline buffer layer on mica. The most promising candidate is the thin film of the layered material. Our group has succeeded in growing good epitaxial films of transition metal dichalcogenides such as MoSe₂ and NbSe₂ on the cleaved surfaces of mica.^{14,15)} These materials have a layered crystal structure¹⁶⁾ similarly to mica or graphite, and their epitaxial growth is achieved by the so-called “*van der Waals epitaxy* (VDWE)” process.^{17,18)} As the buffer layer for OFETs on mica, the layered material film grown by VDWE must have high resistivity; thus, some suitable layered materials must be found. Research is underway to exploit layered materials as a shielding layer for OFETs on mica gate dielectrics.

In summary, we explored the effect of potassium ions in pentacene OFETs fabricated on

a mica gate dielectric by inserting buffer layers of PMMA or OTMS between the substrate and the pentacene active layer. Improvements of OFET performances were achieved by reducing the unfavorable effects of potassium ions on carrier transport in the pentacene channel. A highly ordered OTMS-SAM was found to work as an excellent shielding layer, even though its thickness is much smaller than that of drop-casted PMMA films.

Acknowledgment

This work was supported by a Grant-in-Aid for Creative Scientific Research (No. 14GS0207) and for Scientific Research (C) (No. 17550165) from the Ministry of Education, Culture, Sports, Science and Technology of Japan.

- 1) Y. Sun, Y. Liu, and D. Zhu: *J. Mater. Chem.* **15** (2005) 53.
- 2) A. Facchetti, M. H. Yoon, and T. J. Marks: *Adv. Mater.* **17** (2005) 1705.
- 3) M. Hara, H. Sasabe, A. Yamada, and A. F. Garito: *Jpn. J. Appl. Phys.* **28** (1989) L306.
- 4) M. Sakurai, H. Tada, K. Saiki, and A. Koma: *Jpn. J. Appl. Phys.* **30** (1991) L1892.
- 5) K. Tanigaki, S. Kuroshima, J. Fujita, and T. W. Ebbesen: *Appl. Phys. Lett.* **63** (1993) 2351.
- 6) H. Yamamoto, H. Tada, T. Kawaguchi, and A. Koma: *Appl. Phys. Lett.* **64** (1994) 2099.
- 7) W. Xu and J. G. Hou: *J. Appl. Phys.* **86** (1999) 4660.
- 8) M. Kiguchi, M. Nakayama, K. Fujiwara, K. Ueno, T. Shimada, and K. Saiki: *Jpn. J. Appl. Phys.* **42** (2003) L1408.
- 9) A. Dodabalapur, L. Torsi, and H. E. Katz: *Science* **268** (1995) 270.
- 10) A. Matsumoto, R. Onoki, K. Ueno, S. Ikeda, and K. Saiki: *Chem. Lett.* **35** (2006) 354.
- 11) C. D. Dimitrakopoulos, A. R. Brown, and A. Pomp: *J. Appl. Phys.* **80** (1996) 2501.
- 12) H. Sugimura, K. Hayashi, N. Saito, O. Takai, and N. Nakagiri: *Jpn. J. Appl. Phys.* **40** (2001) 4373.
- 13) Y. Furubayashi, T. Hitosugi, Y. Yamamoto, K. Inaba, G. Kinoda, Y. Hirose, T. Shimada, and T. Hasegawa: *Appl. Phys. Lett.* **86** (2005) 252101.
- 14) K. Saiki, K. Ueno, T. Shimada, and A. Koma: *J. Cryst. Growth* **95** (1989) 603.
- 15) K. Ueno, K. Saiki, T. Shimada, and A. Koma: *J. Vac. Sci. Technol. A* **8** (1990) 68.
- 16) J. A. Wilson and A. D. Yoffe: *Adv. Phys.* **18** (1969) 193.
- 17) A. Koma, K. Sunouchi, and T. Miyajima: *Microelec. Eng.* **2** (1984) 129.
- 18) A. Koma, K. Sunouchi, and T. Miyajima: *J. Vac. Sci. Technol. B* **3** (1985) 724.

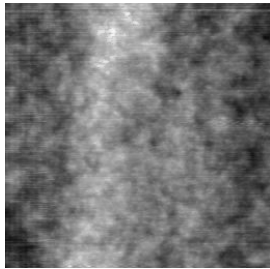
Figure captions

- Fig. 1 AFM images of the substrate and grown films: (a) 85 nm PMMA-coated mica substrate, (b) pentacene film on PMMA/mica substrate, (c) OTMS-SAM-coated mica substrate, and (d) pentacene film on OTMS/mica substrate. All the images show $2 \times 2 \mu\text{m}^2$ scan areas.
- Fig. 2 Transfer characteristics of pentacene OFETs on PMMA/mica substrates as function of thickness of PMMA films. The drain current I_D is normalized; the measured I_D for each sample is divided by the value of gate capacitance per unit area.
- Fig. 3 Output characteristics of pentacene OFETs: (a) on bare mica surface and (b) on 280-nm-thick PMMA-coated mica substrate. The transfer characteristics of both samples are shown in (c).
- Fig. 4 (a) output and (b) transfer characteristics of pentacene OFET on OTMS-SAM-coated mica substrate.
- Fig. 5 Schematics of structure of buffer layers formed on cleaved faces of mica: (a) drop-casted PMMA film and (b) OTMS-SAM. The 2.5-nm-thick OTMS-SAM has a shielding ability that is as good as that of a 280-nm-thick PMMA film.

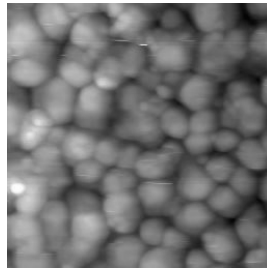
Table I Performances of pentacene OFETs fabricated on mica gate dielectrics with and without PMMA or OTMS buffer films. c_{PMMA} is the wt% concentration of the PMMA solution, t is the thickness of the buffer film, μ is the field-effect mobility, and V_{th} is the threshold voltage estimated from the transfer characteristics. Each on/off ratio was measured at the drain voltage $V_{\text{D}} = 200$ V.

Buffer	c_{PMMA} (%)	t (nm)	μ (cm^2/Vs)	V_{th} (V)	On/off ratio
No buffer		0	8.6×10^{-4}	94	4.5
PMMA	0.5	85	2.7×10^{-2}	120	12
	1.0	140	6.5×10^{-2}	100	16
	2.0	280	1.4×10^{-1}	21	200
OTMS		2.5	3.1×10^{-1}	13	230

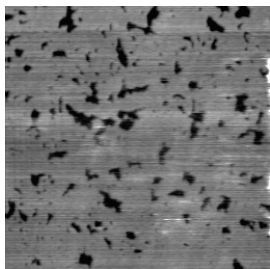
(a) PMMA(85 nm)/mica



(b) pentacene on (a)



(c) OTMS(SAM)/mica



(d) pentacene on (c)

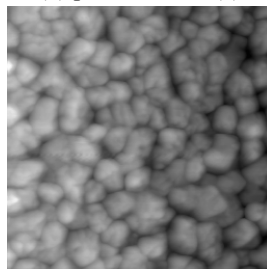


Fig. 1 A. Matsumoto et al.

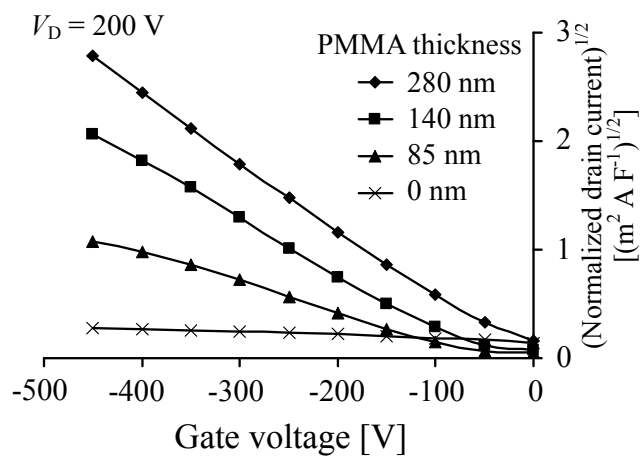


Fig. 2 A. Matsumoto et al.

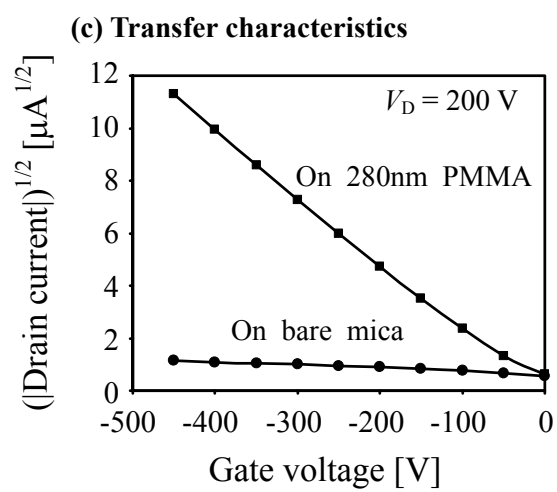
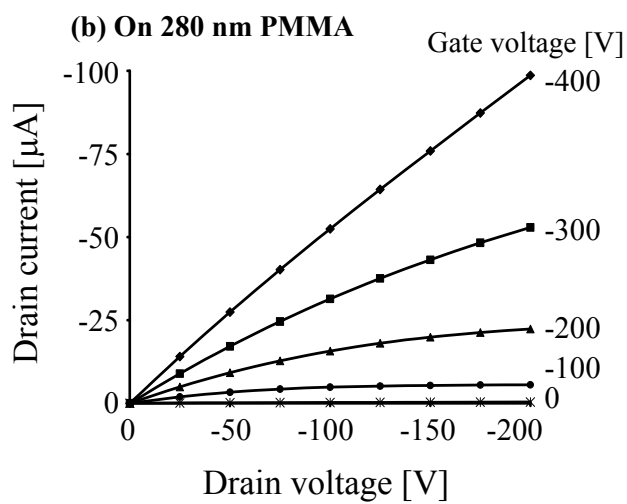
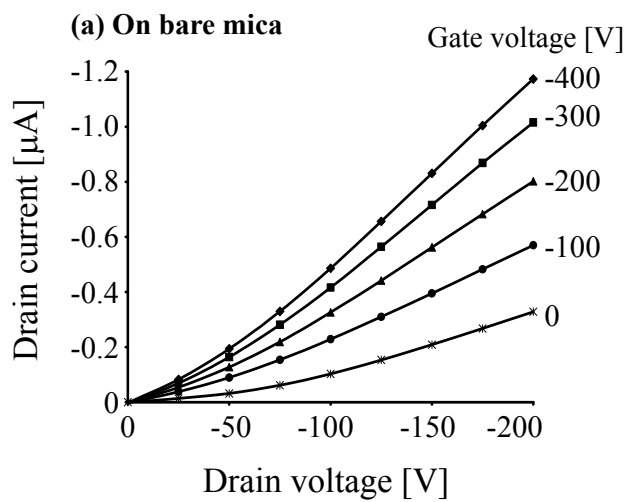


Fig. 3 A. Matsumoto et al.

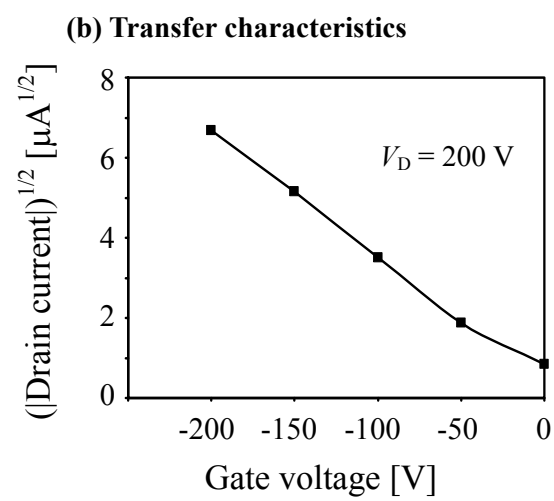
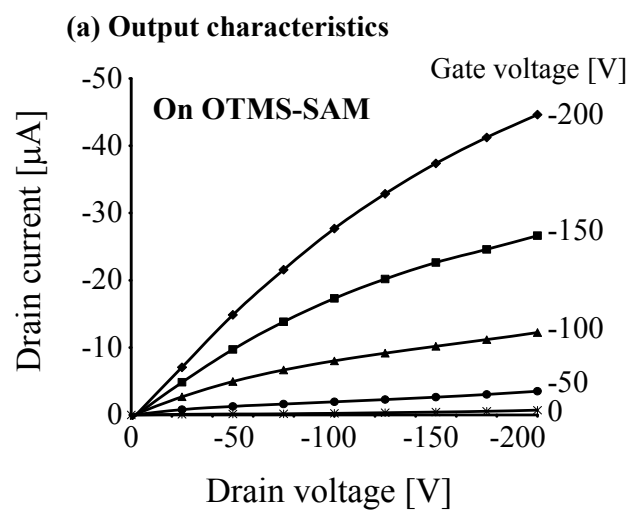


Fig. 4 A. Matsumoto et al.

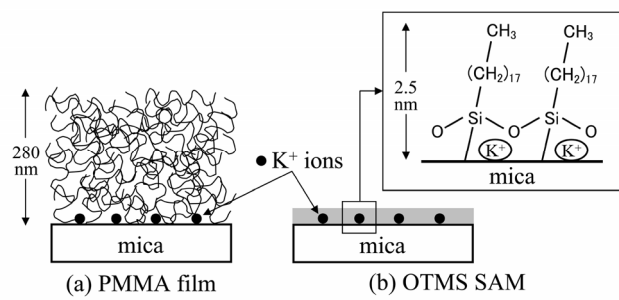


Fig. 5 A. Matsumoto et al.